

Characterization of ZnO Films Doped by Erbium

Valery F. Gremenok^{1,2}, Igor I. Tyukhov³, Neslihan Akcay⁴, Ellen P. Zaretskaya¹,
Vital V. Khoroshko² and Alyaxandr N. Pyatlitski⁵

¹ State Scientific and Production Association "Scientific-Practical Materials Research Centre of the National Academy of Sciences of Belarus", Minsk (Republic of Belarus)

² Belarusian State University of Informatics and Radioelectronics, Minsk (Republic of Belarus)

³ San Jose State University, Department of Mechanical Engineering, San Jose (USA)

⁴ Department of Mechanical Engineering, Faculty of Engineering, Baskent University, Ankara (Turkey)

⁵ JSC «INTEGRAL» – «INTEGRAL» Holding Managing Company, Minsk (Republic of Belarus)

Abstract

Er-doped ZnO thin films were grown on fused quartz and *p*-Si substrates by radio-frequency magnetron sputtering method. The effect of post-deposition treatment at 600 – 900 °C on film properties was studied by scanning electron microscopy, energy dispersive x-ray spectroscopy and atomic force microscopy, X-ray diffraction analysis, optical transmittance, and the room-temperature photoluminescence measurements. All the films showed a (002) preferential orientation with the *c*-axis perpendicular to the substrate surface. The increase of annealing temperature changes some physical properties of ZnO films. The results obtained from both X-ray diffraction and photoluminescence spectra reveal that Er³⁺ ions successfully substitute for Zn²⁺ ions in the ZnO lattice. No impurity phase was found in Er-doped films. The doped ZnO films showed good transmittances (70–80%) in the spectral range of 370-2500 nm. Transmission spectra of as-deposited Er-doped ZnO films contain a wide absorption band in the near-infrared region. Photoluminescence spectra depend on the annealing temperature of films. The appearance of an emission in the visible-near-infrared spectral range occurred. It was found that an increase in the annealing temperature leads to an increase in the photoluminescence intensity in the spectral range of 1.5 - 3.0 eV. Photoluminescence excitation spectra of Er-doped ZnO films contain a band with a maximum at ~ 3.40 eV which corresponds to the band gap energy of ZnO. Hot-Probe characteristics measured for as grown and Er-doped thin films showed that these materials have *n* type conductivity.

Keywords: ZnO thin films, erbium, magnetron sputtering, structural properties, photoluminescence

1. Introduction

Zinc oxide (ZnO) is a wide-gap semiconductor material that possesses a unique combination of optical, acoustic, and electrical properties and is extensively used in a number of optoelectronic devices, such as converters of surface acoustic waves (SAWs), solar cells, optical waveguides, laser reflectors, broadband filters, and liquid-crystal displays (LCDs) (Coleman et al., 2006; Mishra et al. 2015; Wang, 2004). This growing interest in ZnO stems from the possibility to use it in optoelectronics applications, which is made possible mainly due to its direct band gap of $E_g \sim 3.3 - 3.4$ eV at 300 K. It crystallizes at relatively low temperatures, easily processed utilizing chemical etching and has tunable properties by doping to achieve high optical transmittance and low resistance (Nickel and Terukov, 2005). It is known that ZnO exhibits two luminescence bands: a short wavelength band (UV region) and a broad long-wavelength band with the maximum in the green spectral range. The former is due to exciting recombination, whereas the latter is caused by native defects. The contribution of each recombination channel depends on the structural quality and fabrication conditions of ZnO materials. However, the monitoring of visible photoluminescence (PL) is challenging up to now. One of the ways to obtain controllable PL in a specific spectral range is doping with different elements. Additionally, the wide band gap of ZnO allows incorporating luminescent centers such as rare earth (RE).

In recent years, the interest in preparing ZnO thin films doped with lanthanide elements (Ln³⁺) has increased due to the interesting properties that can be obtained by using 4f valence electron elements (Akazawa et al., 2014, Das et

al., 2015, Kumar et al., 2017). It is well known that rare-earth ions (erbium, terbium, europium, thulium, and so on) are a special kind of photoactive centers with narrow emission lines and long emission lifetimes in various semiconductor materials. The trivalent rare earth (RE) elements have been tested as dopants resulting in high ZnO film conductivity and specific luminescence properties (Kumar et al., 2017). Among them, erbium (Er^{3+}) is a suitable candidate for the conversion of infrared to visible light due to its favorable electronic energy level structure (Akazawa and Shinojima, 2014; Kohls et al., 2002; Meng et al., 2011; Schmidt et al., 1998). Trivalent erbium has an incomplete 4f electronic shell that is shielded from the outer atomic environment by closed 5s and 5p shells. As a result, rather sharp optical intra-4f transitions can be achieved from erbium doped materials. The transition from the first excited state to the ground state in Er^{3+} occurs at an energy of 0.8 eV, corresponding to a wavelength of 1.54 μm . This is an important telecommunication wavelength since standard silica-based optical fibers have their maximum transparency at this wavelength and extensively used as an eye-safe source in the atmosphere, laser radar, medicine, and surgery (Kenyon, 2002; Kumar et al., 2017). The studies of Er-doped ZnO (ErZO) thin films showed that the 1.54 μm luminescence would occur when the Er atoms are triply ionized and embedded in the ZnO hosts. It is allowing an effective energy transfer from the excited host electrons in the conduction band to the Er ions - a common indirect excitation mechanism for Er doped semiconductors (Polman, 1997). It has been demonstrated that Er acts as an optically active center if it is surrounded by oxygen forming a pseudo-octahedron structure (Kenyon, 2002; Kumar et al., 2017). This means that Er replacing Zn in the ZnO matrix forms Er_2O_3 and does not act as an optically active center. Therefore, an annealing treatment of thin films is required to change local structure of Er, forming clusters either in the ZnO matrix or at the grain boundaries.

Thin film growth parameters are largely affected by the deposition techniques and the process parameters. There are various deposition techniques available for preparing ZnO thin film (Coleman et al., 2006; Mishra et al. 2015; Wang, 2004). One of the methods for ZnO film fabrication is radio-frequency (RF) magnetron sputtering. It results in the formation of columnar ZnO film with a preferred orientation of c-axes perpendicularly to the substrate surface. However, comparison of the results obtained for thin films, as far as we know, sometimes is contradictory. At the same time, the type of substrate can affect the structure as well as Er incorporation into ZnO grains. Another important factor is the growth and annealing temperature for thin film formation.

In this work, the Er-doped ZnO films were grown on fused quartz and *p*-Si substrates by radio-frequency magnetron sputtering and the effect of thermal annealing at 600 – 900 °C on their structural and optical properties was investigated aiming at the fine-tuning of RE ion emission.

2. Experimental

ErZO thin films were grown by RF magnetron sputtering of nominally pure Zn and ErCl_3 -targets in an argon atmosphere with oxygen (20% Ar and 80% O_2) at a pressure of 5×10^{-3} Torr on pure Si and fused quartz substrates. We used targets with erbium composition of 1% and 2% by mass. The power density applied to the cathode was 2.0 W/cm^2 and the deposition time was 60 min. Both types of substrates were placed on the same sample holder to obtain the layers grown under the same conditions. The substrate temperature was kept at 25 °C. Si wafers were etched in 10%-water HF solution to remove the thermal SiO_2 layer from their surface. Before the deposition, all substrates were submitted to the cleaning procedure in an ultrasonic bath for 5 min to remove mechanical pollution, then sent to cleaning in propanol for 5 min and drying with nitrogen flow. The thickness of all films investigated was about 600 - 700 nm. After the deposition, the wafers were cut into $1 \times 1 \text{ cm}^2$ pieces. Isochronal (30 - 150 min) post-growth annealing was performed at 600, 750, and 900 °C in a conventional furnace in nitrogen flow.

XRD measurements of ZnO films were performed using Ultima IV X-ray diffractometer (Rigaku) in grazing incidence X-ray diffraction (GIXD) geometry at 1.0° of incident X-rays with $\text{CuK}\alpha$ radiation source scanned in the range of $10 - 80^\circ$ at room temperature. The evaluation of the XRD spectra of the films was conducted using JCPDS data cards. Chemical composition and the depth profile of elements in the films were determined by energy dispersive X-ray spectroscopy analysis (EDX) and Auger electron spectroscopy (AES) using a CAMECA SX-100 and Perkin Elmer Physics Electronic 590, respectively. An Ar ion beam with energy of 5 keV was used for simultaneous sputter etching. Morphology was analyzed by scanning electron microscopy (SEM) using the JEOL 6400. The AFM experiments were carried out in Intermittent contact mode, using a Solver Nano, NT-MDT atomic force microscope with a $10 \mu\text{m} \times 10 \mu\text{m}$ high resolution scanner with a vertical range of 2 μm , z-axis resolution 0.027 nm, and an X-Y linearity mean error of less than 0.6 %. Sharp tips were employed for measurements; with a radius of curvature of less than 10 nm. Topographic 2D AFM images have been recorded with a resolution of 256×256 pixels over scanning areas of $4 \times 4 \mu\text{m}^2$ and the Nanosurf Easyscan2 software program (v1-6-0-0) was used for image processing and roughness evaluation. The transmittance (T) spectra of the ErZO thin films onto quartz substrates were measured in the spectral range of 200 – 3000 nm using a Carry 500 Scan UV-Vis-NIR (Varian, USA) spectrophotometer.

Photoluminescence (PL) and photoluminescence excitation (PLE) measurements were carried out by employing a 1000 W Xe lamp as an excitation source combined with a grating monochromator (600 grooves/mm, focal length ~ 0.3 m). All measurements were performed at room temperature. The Hot Probe characterization method was used for the definition of a semiconductor type, *p* or *n*, for as grown and ErZO thin films.

3. Results and discussion

3.1. Elemental composition and morphology of the films

The composition of the thin films before and after the annealing was estimated from the EDX measurements and appeared to be invariable after the heat treatment. The chemical composition was determined by averaging the concentration values from 10 different points on the surface of the same film (Tab. 1). The EDX results show that the incorporation coefficient for Er⁺³ ions is low and reach approximately 1.5 %. The EDX spectrum of Er-doped films shows the signals of Zn, O, Er, Si, C, and Ca where the signals of Si, C, Ca are from the substrates. Elemental mapping of Zn, Er, and O, shows a homogeneous distribution of all components without any concentrated places at the surface (not shown here).

Tab. 1: - Chemical composition of as-grown films i-ZnO and ErZO:Er films doped by erbium fabricated on silicon and fused quartz substrates

Sample	Substrate	Annealing temperature, °C	Zn, at. %	O, at. %	Er, at. %
i-ZnO	Si	25	49.9	50.1	
1-ErZO	Si	25	48.7	50.5	0.8
2-ErZO	Si	600	49.1	50.1	0.8
3-ErZO	Si	900	49.3	50.0	0.7
4-ErZO	quartz	25	49.2	49.3	1.5
5-ErZO	quartz	600	49.5	49.1	1.4
6-ErZO	quartz	900	49.1	49.4	1.4

A similar elemental composition (Zn, O, Er in atomic %) of ZnO thin films has been confirmed by AES method. The spectra were analyzed over a range of kinetic energies from 100 to 1400 eV using the primary electron beam of energy 5.0 keV. As an example, Fig. 1 shows the depth profile of elements for the as-grown non-annealed 1-ErZO film. The homogeneous distribution of all elements Zn, O, and Er along the depth of films is seen from Fig. 1. A similar homogeneous elements distribution is also revealed for all investigated films on different substrates. This fact confirmed the high-quality of the deposited films with nearly ideal stoichiometry of Zn and O chemical elements. The measurements show that Er atomic concentration in ZnO is not exceeded 1.5 at. % at magnetron sputtering. The surface morphology and cross-section images of the thin films were characterized by SEM. According to crystal growth mechanisms, the growing faces of crystallites correspond to the crystal shape at equilibrium and are determined by the orientation of the crystal. A growth competition can start among the neighboring crystals according to their orientation. The faster-growing crystals will grow over slower-growing ones. Once the competition proceeds towards the formation of the same type of crystal faces, they form the free surface. This competitive growth mode represents an orientation selection resulting in the competitive growth texture. For ZnO, stably preferential orientation is along to *c*-axis (Coleman et al., 2006). The thermodynamically stable phase of ZnO is wurtzite symmetry. From the cross-section SEM images (Fig. 2), Er-doped ZnO films exhibit good flatness and the crystal grain size is dependent on the substrate (silicon, quartz) and the deposition conditions.

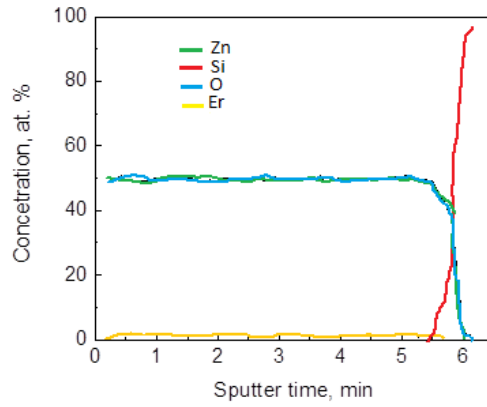


Fig. 1: AES depth profile of chemical elements of ErZO films on silicon substrate

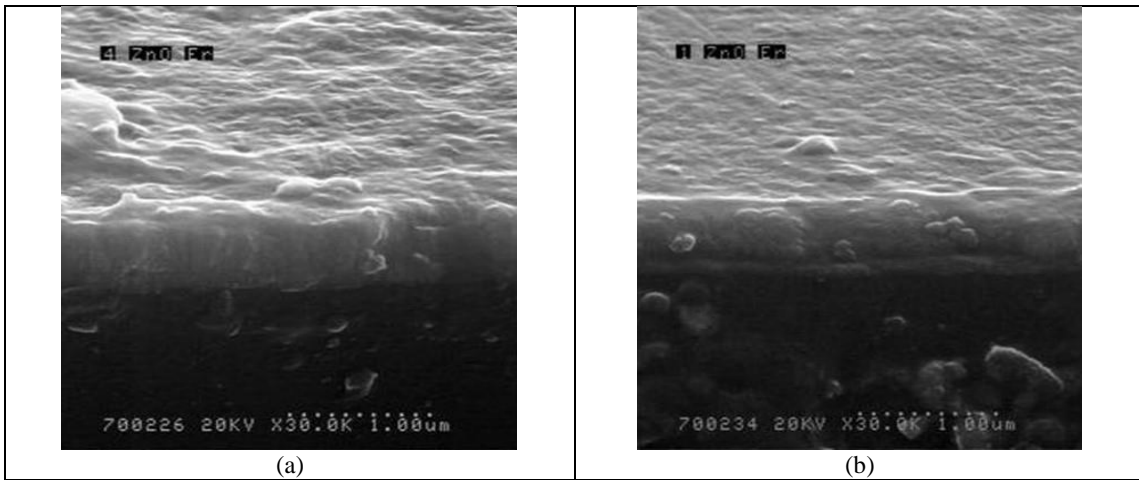


Fig. 2: Cross-section SEM images of as-grown ErZO films on quartz (a) and silicon (b) substrates

As seen the films are consisting of grains with a size of about 0.10 – 0.15 μm with the well-faceted structure without any porous, nearly smooth surface and the crystal grain size is dependent on the Er concentration. The ZnO:Er films fabricated on fused silica substrates consist of separate nanocrystallite with a bigger size. The difference in the morphology of as-grown and Er doped ZnO films after the annealing is reflected by the size and shape of grains. The films do not have a large number of grain boundaries due to the absence of Er ions at the grain boundaries. The annealing might have helped the grains to grow much bigger, since high-temperature annealing stimulates the migration of grain boundaries and causes the coalescence of more grains. Good crystallinity should help improve the optical and electrical properties of the films.

Fig. 3 shows the AFM images taken on the ZnO films with different Er concentration. As can be seen from the AFM images, the coatings produced in all types of reagents are continuous, with no visible pores or puncturing, and formed of pyramidal crystallites grown along the same direction orthogonal to the substrate surface.

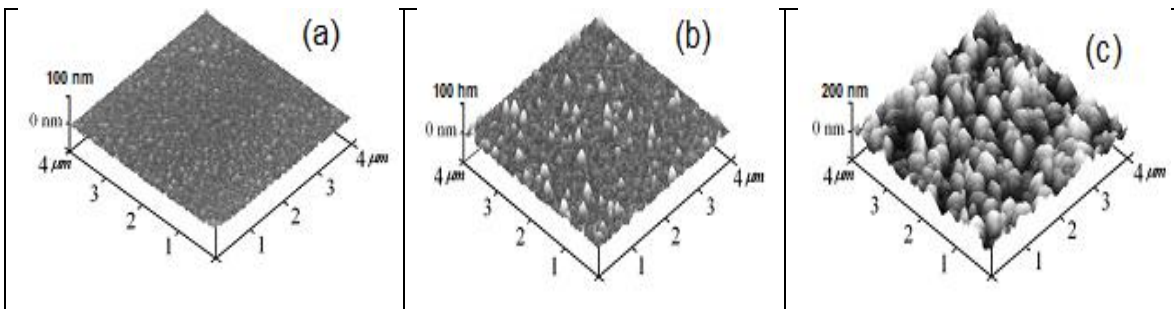


Fig. 3: AFM images, at the scale of $(4 \times 4) \mu\text{m}^2$, of (a) i-ZnO, (b) 1-ErZO and (c) 5-ErZO thin films

The increasing of the grain size of ZnO thin films prepared on different substrates with increasing Er concentration is clearly observed. The root mean square (RMS) roughness is 7.42, 12.26, and 26.73 nm for the films with Er concentration of 0.0 %, 0.8 %, and 1.5 %, respectively. Most probably the roughness increases could be related to the increasing of surface defects (such as valleys and hills) after layer depositions and thermal treatments.

3.2. X-ray diffraction (XRD) analysis

The typical XRD patterns of ErZO thin films are shown in Fig. 4(a). The scans for the films grown onto different substrates demonstrate two peaks at $2\theta \sim 34.5^\circ$ and 72.4° , respectively. These peaks are caused by reflection from (002) and (004) planes of hexagonal phase crystalline ZnO (JCPDS 36-1451 card).

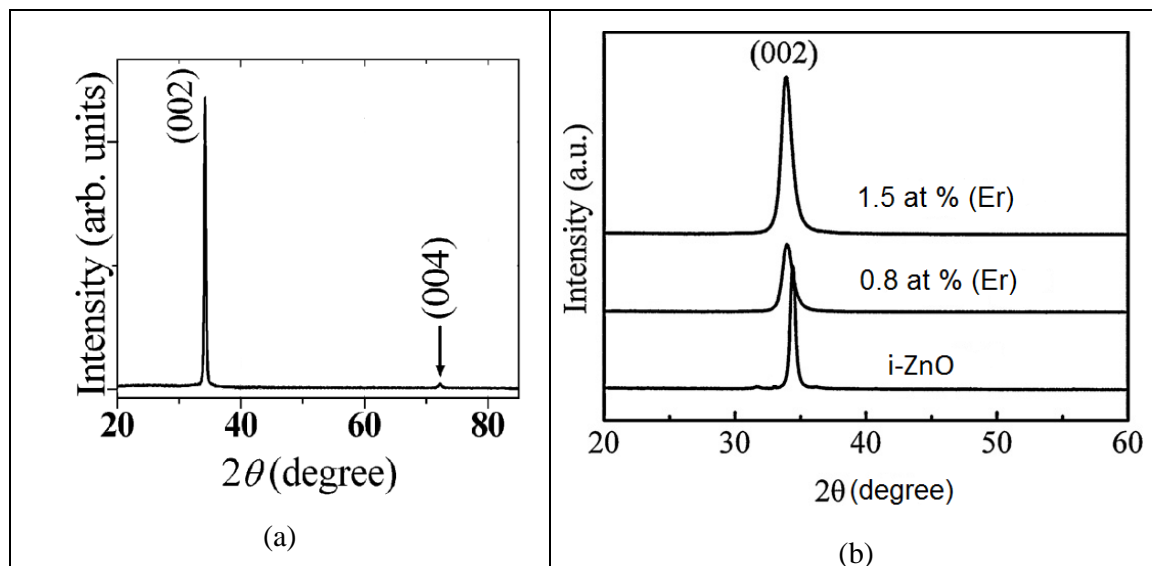


Fig. 4: Typical X-ray of powder diffraction pattern of ErZO thin films on different substrates (a) and XRD peak position (c) in dependence on the Er concentration (b)

The greater intensities of (002) peaks in respective patterns indicated that crystallites grow preponderantly oriented with *c*-axis normal to the substrate (column-like structure). As it is shown in (Coleman et al., 2006; Wang, 2004) the film grains, after their coalescence, grow mainly in the direction normal to the substrate surface. In the case of hexagonal crystalline structure, this direction will be one. Most of the closely packed structures have the lowest free surface energy in the (002) plane and crystallization favorably occurs in this direction. Experimental data indicate that single phase ErZO layers without any second crystalline phase, such as free Er or erbium oxide, in particular, Er_2O_3 may be fabricated under technological conditions. The as-deposited ZnO films did not show any feature related to the Er_2O_3 phase, suggesting that Er atoms are either substitutionally replacing Zn in the ZnO lattice or segregated to the non-crystalline region in grain boundaries (Polman, 1997; Kenyon, 2002). Fig. 4(b) shows, that the (002) XRD peaks with the increasing Er concentration are shifted towards lower angles with respect to that for pure ZnO ($2\theta = 34.42^\circ$). Films had '*c*' parameter values slightly higher than that of ZnO powder material ($c = 0.521$ nm), indicating that the unit cells of thin films are elongated along the *c*-axis and the compressive forces were predominant. The '*c*' lattice constant increases from 5.21 Å to 5.28 Å with increasing Er concentration from 0.0 to 1.5 at. %. As the ionic radius of Er^{3+} (0.89 Å) is larger than that of Zn^{2+} (0.74 Å) (Polman, 1997), the increase of this '*c*' lattice constant indicates that Er^{3+} ions successfully substitute for Zn^{2+} ions in the ZnO lattice. The internal compressive stress in the films is assigned to the bombardment of energetic particles during the deposition and not to the thermal stress originating from the difference between the thermal expansion coefficient of the film and the substrate (Coleman et al., 2006; Nickel and Terukov, 2005).

On the other hand, when the samples were annealed, the microstructure of the films was not changed by the plausible oxidation of Er and presented the Er_2O_3 phase in the XRD patterns. The presence of the Er_2O_3 phase was not observed in the sample, associated either with the relatively small amount of Er atoms incorporated into the film (low doping level) or due to the absence of those phases for the employed deposition conditions. After the annealing, the peaks were shifted to higher diffraction angles and the films showed lattice parameters (*a* and *c*) slightly lower than the ideal values for undoped ZnO films. This suggested that the stress was changing from compressive to tensile. It is possible that the annealing temperature produced tensile stress due to the mismatch between thermal energy

coefficients when the films cooled down (Hodes, 2005). It was also observed that the annealing of films produces variation in the intensity of the main diffraction peak (002) and showed an increase in its intensity, which unequivocally indicates an enhancement of the film's crystalline arrangement. The average crystallite size in the direction of normal to the reflecting planes was increased after the annealing process.

3.3. Optical and photoluminescence study

With the aim of the band gap energy determination of different ErZO films fabricated on quartz substrates the measurements of reflectance spectra at room temperature have been performed. As an example, Fig. 5 shows transmission spectra of thin films prepared on these substrates.

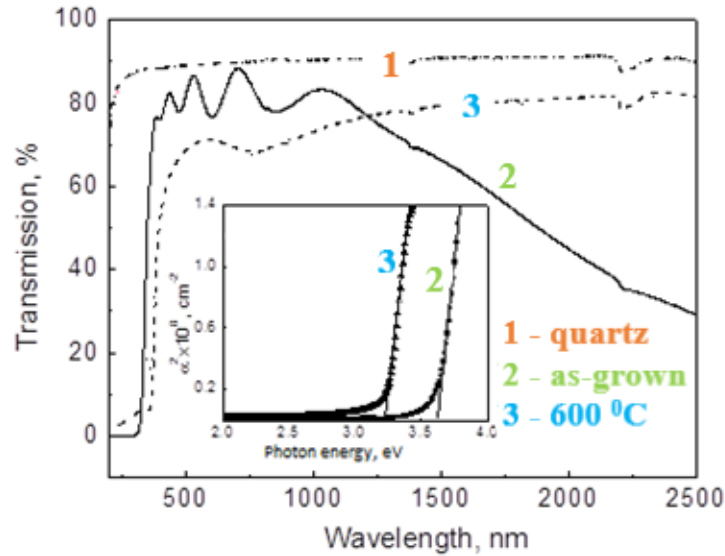


Fig. 5: Transmission spectra and the dependence of α^2 vs $h\nu$ for ErZO films on quartz substrates

As seen all films have a high value of transmittance $\sim 70 - 80\%$ in wide spectral range 370-2500 nm, intensive interference fringes, and a relatively sharp edge of the intrinsic absorption which starts at less than 390 nm. The sharp decrease in the transmission spectrum below ~ 450 nm is related to the strong absorption of the photons in this region. Besides the interference fringes arising at the reflection from boundaries of a film-substrate and a film-air, the wide absorption band from 1.0 to 2.5 μm in the IR range of a spectrum, is seen. These experimental data confirmed the high quality of ErZO layers grown on quartz substrates. The shifting of intrinsic band edge in the ultraviolet spectral region and decreasing transmittance in the near-infrared region is observed for no annealed films in contrast to i-ZnO films. The absorption in 1.0 – 2.5 μm spectral region and high-energy shift of absorption edge are indicating strong doping effect of ZnO films by Er atoms. A similar behavior of optical spectra is observed for n-type highly doped semiconductors such as ZnO:Al (Coleman et al., 2006; Nickel and Terukov, 2005). This phenomenon may be explained by the Burstein-Moss effect. As seen, annealing at temperatures higher than 600 °C leads to a low-energy shift of intrinsic absorption edge and decrease in infrared absorption.

The transmission spectra presented in Fig. 5 were analyzed under the light of Tauc expression and the derivative spectroscopy technique. The absorption coefficient (α) was calculated by the expression of $\alpha = -\ln \tau/d$, where the film thickness is $d \approx 700$ nm. Tauc formula is related with the band gap energy (E_g) and the absorption coefficient (Pankove, 1971):

$$(\alpha h\nu) = A(h\nu - E_g)^n, \quad (\text{eq. 1})$$

where A and n are band tailing parameters and index, respectively. The n index is 2 for indirect and 1/2 for direct band gap energy characteristics. The Eq. (1) states that $(\alpha h\nu)^{1/n}$ vs. $(h\nu)$ plot exhibits a linear region in the strong absorption region. The linear fitted line intersects the energy axis at the band gap energy value. The $(\alpha h\nu)^2$ vs. $(h\nu)$ plots for ErZO films are shown in the inset of Fig. 5. Determination of E_g value is illustrated in the inset of Fig. 5 and it amounts to 3.62 eV and 3.22 eV for the as-deposited (4-ErZO) and after annealing (6-ErZO) films, respectively. These values are consistent with that measured from PLE spectra for the same samples.

The main attention was concentrated on the photoluminescence and photoluminescence excitation measurements of ZnO films prepared on different substrates. As an example, Fig. 6 shows the photoluminescence and photoluminescence excitation spectra of i-ZnO thin films grown on p-type Si substrate after 30 min and subsequent

annealing at temperatures of 600 °C, 750 °C, and 900 °C. The PL and PLE spectra were taken at room temperature. It is clearly seen that PL spectra contain two broad intense bands with maxima at 2.43 eV (green emission 510 nm) and at 1.94 eV (yellow emission at 640 nm). The experiments show that the relative intensity of green and yellow emissions increases with annealing temperature reaching a maximum at 900 °C.

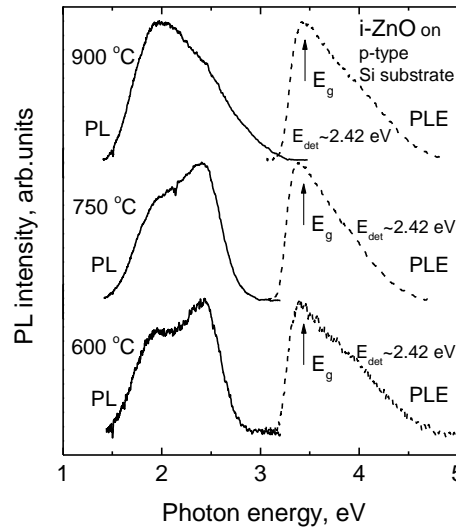


Fig. 6: PL and PLE spectra of i-ZnO thin films for different annealing temperature

The annealing time in the range from 30 up to 150 min for each temperature, as indicated in Fig. 6, also increases the intensity of the bands at 2.43 eV and 1.94 eV. These two bands may be referred to oxygen vacancy (V_{O}^+) and oxygen interstitial (O_i^-) respectively. The changes in the relative intensity of both bands are observed at annealing temperature variation. This effect indicates redistribution of radiative recombination channels of nonequilibrium charge carriers. Fig.6 shows that the green-dominant emission at lower annealing temperature (600 and 750 °C) is switched to yellow emission at higher annealing temperature (900 °C). This is issued by the competition between the formation of V_{O}^+ and O_i^- defects. A broad PLE band with a maximum at 3.40 eV was observed for all investigated i-ZnO films. The energy maximum at $3.40 \text{ eV} \pm 0.05 \text{ eV}$ corresponds to the optical band gap energy of ZnO material. Fig. 7 shows the PL spectra taken at room temperature for Er-doped ZnO thin films on Si substrate. The deposited films were annealed at different temperatures. When the annealing temperature increased in the range 600 – 900 °C high strength deep-level emission in the spectral region 1.5 – 3.0 eV has been observed.

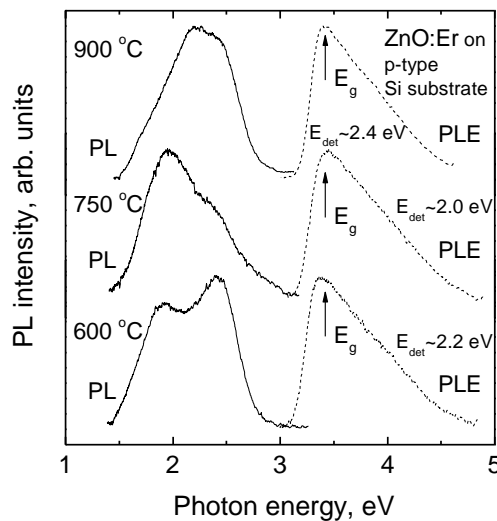


Fig. 7: PL and PLE spectra of ErZO thin films for different annealing temperature

It can be seen that the peak intensity and energy position of deep-level emission varies with annealing temperatures. In particular, ErZO films annealed at 900 °C show only one broad PL band. The appearance of this band may be related to the formation of defects induced by Er atom incorporation in the ZnO lattice. The rate of formation point

defects is low for ErZO films annealed at low temperature ~ 600 °C. More defects responsible for the radiative transitions introduce into the films for the temperatures higher than 600 °C. In addition to thermal treatment, doping by Er atoms plays an important role in the mechanism responsible for the deep-level luminescence as well. It is notable that the yellow emission decreases with increasing annealing temperature for Er-doped ZnO thin films. One cause is most likely due to the formation of Er - V_O bonds in ErZO films. Another possibility of the variation in the intensity of the yellow band at ~ 1.94 eV can be ascribed to the additional formation of interstitial oxygen. The probability of the electron charge transfer from localized impurity states to the conductive states is increased due to the potential fluctuation of Er impurities in ZnO films. We must speculate that both probable mechanisms are responsible for the increase of green emission. Further investigations are needed to verify this point of view. The PLE spectra of Er-doped films also contain broad band with a maximum at 3.40 ± 0.05 eV which corresponds to the optical band gap energy of ZnO.

It is well known that Er^{3+} ions (Polman, 1997; Kenyon, 2002; Kumar et al., 2017) are responsible for the visible luminescence in the spectral region 500 – 600 nm (2.07 – 2.48 eV). We cannot have detected sharp Er^{3+} related lines in the green region of spectra due to high-intensity emission related to intrinsic point defects such as O_i and V_O in ZnO material. Instead that we detected infrared luminescence of erbium in ZnO films (Fig. 8-9).

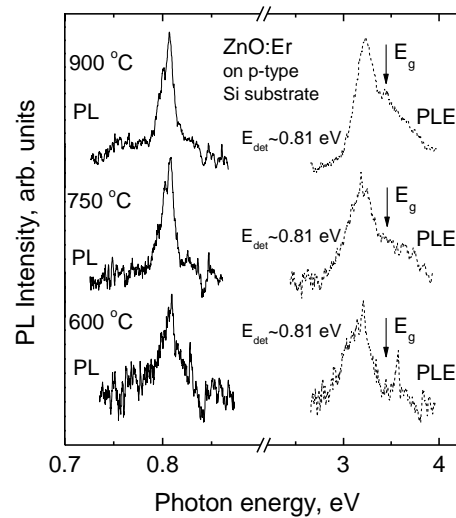


Fig. 8: PL and PLE spectra of ErZO thin films for different annealing temperature

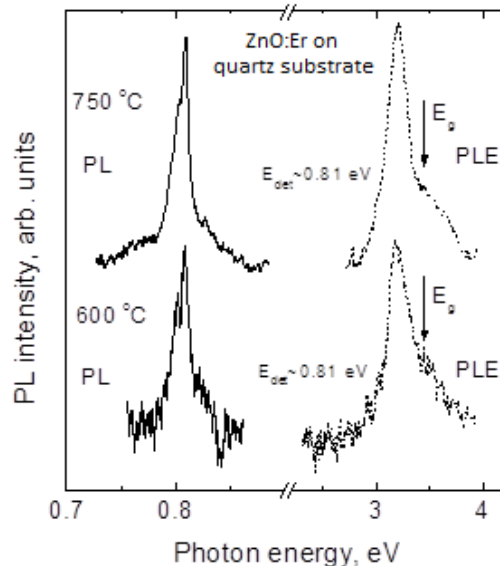


Fig. 9: PL and PLE spectra of ErZO thin films on quartz substrate for different annealing temperature

It is clearly seen that ErZO films exhibited 1.54 (0.81 eV) μm Er^{3+} photoluminescence (Schmidt et al., 1998, Wang et al., 2006). This fact strongly suggests that Er^{3+} ions were incorporated in the ZnO lattice during the magnetron

sputtering process. The Er emission mechanism under indirect excitation is generally explained using an energy transfer model (Kenyon, 2002; Kumar et al., 2017). In the thin film and/or bulk counterparts of Er doped ZnO, the necessity of annealing to obtain the 1.54 μm luminescence is explained by Er site activation. It has been found that the higher order O coordination around the Er decreased the PL intensity, which could be significantly improved when the local structure of the Er–O cluster changed to a pseudo-octahedron with C_{4v} symmetry (Ishii, 2001).

The PLE spectra of the infrared luminescence of Er-doped ZnO films on different substrates as a function of excitation wavelength showed that infrared Er^{3+} related emission may be excited by the band-to-band mechanisms in ZnO material as well as upper above gap excitation (Fig 8-9). The relatively intense broad band at 3.2 eV has been found in the PLE spectra for the different stages of the annealing.

A more interesting experimental finding is the efficient excitation of Er^{3+} -related emission near 1.54 μm (0.81 eV) throughout the band at 3.2 eV in comparing with band-to-band optical transition in PLE spectra of ErZO thin films. The band at 3.2 eV in PLE spectra (Fig. 8 and Fig. 9) may be attributed to the optical transitions on Er-O defects with relatively shallow energy levels in thin films (Polman, 1997; Kenyon, 2002; Kumar et al., 2017). An increase in the intensity of the PLE band at 3.2 eV with increasing annealing temperature results from the increasing concentration of structural Er – O defects and the formation of impurity energy band with shallow levels.

The conventional Hot Probe characterization method was used for the definition of a semiconductor type, *p* or *n*, by identifying the majority of the charged carriers by the sign of the measured voltage. Hot-Probe characteristics measured for as grown and ErZO thin films demonstrated that these materials have *n* type conductivity.

4. Conclusions

The effect of different atomic contents of Er^{3+} ions on structural, optical, and photoluminescence properties of ZnO films grown on fused quartz and *p*-Si substrates was studied by different experimental techniques. All investigated films were found by XRD to have a polycrystalline wurtzite type structure and exhibit (002) preferential orientation with the *c*-axis perpendicular to the substrate surface. As the annealing temperature increased, some changes in the physical properties have been observed. The change of the lattice parameters indicates that dopant ions substituting Zn ions were incorporated into the ZnO lattice. The doped ZnO films showed good transmittances (70–80%) in the spectral range of 370-2500 nm. Transmission spectra of as-deposited Er-doped ZnO films contain a wide absorption band in near-infrared region. The annealing at temperatures higher than 600 °C in nitrogen flow of these films leads to the disappearance of this band and to a low-energy shift of intrinsic absorption edge. After post-annealing treatment of ErZO films green and near 1.54 μm PL emission related to intra-4f shell of Er^{3+} ions is observed. The relatively intense broad band at 3.2 eV has been found in the PLE spectra for the different stages of the annealing and may be attributed to the optical transitions on Er-O defects with relatively shallow energy levels in ZnO:Er material. The PLE spectra of ErZO thin films on different substrates also contain broad band with a maximum of 3.40 ± 0.05 eV which corresponds to the band gap energy of pure ZnO. As grown and Er-doped films have *n* type conductivity. Our results indicate that Er^{3+} ions are an effective co-doping element for ZnO films which can be used for application in thin film devices, laser and display technologies. The high structure quality of the Er doped thin films and the room temperature 1.54 μm (0.81 eV) luminescence make them promising candidate to serve as functional units for applications in future optical communications.

5. Acknowledgments

Financial support from the Belarusian Republican Foundation for Fundamental Research, grant № T20UK-022, is gratefully acknowledged. The part of the work has been financed by the Belarusian State Programme for Research «Physical Material Science, New Materials and Technologies». The authors of this work are grateful to Affiliate RDC “Belmicrosystems” JSC “INTEGRAL”-“INTEGRAL” Holding Managing Company for EDX and SEM studies of thin films.

6. References

- Akazawa, H., Shinojima, H., 2014. Relation between process parameters of ZnO host films and optical activation of doped Er^{3+} ions. Mater. Sci. Eng. B. 189, 38–44.
- Coleman, V.A., Victoria, A., Jagadish, C., 2006. Basic Properties and Applications of ZnO, Zinc Oxide Bulk, Thin Films and Nanostructures, Elsevier Science Ltd, Amsterdam.
- Das, R., Khichar, N., Chawla, S., 2015. Dual Mode Luminescence in Rare Earth ($\text{Er}^{3+}/\text{Ho}^{3+}$) Doped ZnO Nanoparticles Fabricated by Inclusive Coprecipitation Technique. J. Mater. Sci.: Mater. Electron. 26, 7174–7182.

- Hodes, G., 2005. Chemical Solution Deposition of Semiconductor Films, Marcel Dekker, Inc, New York.
- Ishii, M., Komuro, S., Morikawa, T., Aoyagi, Y., 2001. Local structure analysis of an optically active center in Er-doped ZnO film. *J. Appl. Phys.* 89, 3679-3684.
- Kenyon, A.J., 2002. Recent developments in rare-earth doped materials for optoelectronics. *Prog. Quantum Electron.* 26, 225–284.
- Kohls, M., Bonanni, M., Spanhel, L., Su, D.S., Giersig, M., 2002. Green Er^{III} Luminescence in Fractal ZnO Nanolattices. *Appl. Phys. Lett.* 81, 3858-3860.
- Kumar, Vinod, Ntwaeaborwa O.M., Soga T., Dutta Viresh, and Swart H.C., 2017. Rare Earth Doped Zinc Oxide Nanophosphor Powder: A Future Material for Solid State Lighting and Solar Cells. *ACS Photonics.* 4, 2613–2637.
- Meng, X., Liu, C., Wu, F., and Li, J., 2011. Strong up-conversion emissions in ZnO:Er³⁺, ZnO:Er³⁺-Yb³⁺ nanoparticles and their surface modified counterparts. *J. Colloid Interface Sci.* 358, 334–337.
- Mishra, Y.K., Modi, G., Cretu, V., Postica, V., Lupan, O., Reimer, T., Paulowicz, I., Hrkac, V., Kienle, L., Adlung, R., 2015. Direct growth of freestanding ZnO tetrapod networks for multifunctional applications in photocatalysis, UV photodetection, and gas sensing. *ACS Appl. Mater. Interfaces.* 7, 14303–14316.
- Nickel, N.H., Terukov, E., 2005. Zinc Oxide - A Material for Micro - and Optoelectronic Applications, Springer, Netherlands.
- Polman, A, 1997. Erbium implanted thin film photonic materials, *Journal of Applied Physics.* 82, 1–39.
- Pankove, J.I., 1971. Optical Processes in Semiconductors, Prentice-Hall, Englewood Cliffs, New Jersey.
- Schmidt, T., Muller, G., Spanhel, L., Kerkel, K., Forchel, A., 1998. Activation of 1.54 μm Er³⁺ Fluorescence in Concentrated II–VI Semiconductor Cluster Environments. *Chem. Mater.* 10, 65–71.
- Wang, X., Kong, X., Shan, G., Yu, Y., Sun, Y., Feng, L., Chao, K., Lu, S., Li, Y., 2004. Luminescence Spectroscopy and Visible Upconversion Properties of Er³⁺ in ZnO Nanocrystals. *J. Phys. Chem. B.* 108, 18408–18413.
- Wang, Juan, Zhou, M.J., Hark, S.K., Lia, Quan, Tang, D., Chu, M.W., Chen, C.H., 2006. Local electronic structure and luminescence properties of Er doped ZnO nanowires. *Appl. Phys. Lett.* 89, 221917.
- Wang, Z.L., 2004. Zinc oxide nanostructures: growth, properties and applications. *Journal of Physics: Condensed Matter.* 16, R829–R858.